# Clutter-Based Evaporation Duct Estimation Performance Using Meteorological Statistics

***Caglar Yardim, Peter Gerstoft, and William S. Hodgkiss***

Marine Physical Laboratory
University of California, San Diego
La Jolla, CA 92093–0238, USA
(email: cyardim@ucsd.edu, gerstoft@ucsd.edu, whodgkiss@ucsd.edu)

## Abstract

This paper addresses how to assess the performance of refractivity-from-clutter (RFC) techniques in different regions of the world with varying duct strengths and statistics. The performance of evaporation duct estimation is investigated in littoral zones such as the North Sea, Wallops Island, Coast of California, Mediterranean, Persian Gulf, and Coast of Brazil. The effects of the radar frequency (S, C, and X bands), antenna height, and the complex interaction of these factors with meteorological statistics are studied. An evaporation duct inversion performance map of the Space Range Radar (SPANDAR) is created for the larger Mediterranean/Arabian Sea Region.

## 1 Introduction

In many maritime regions of the world, such as the Mediterranean, Persian Gulf, East China Sea, and California Coast, atmospheric ducts are common occurrences. They result in various anomalies such as significant variations in the maximum operational radar range and increased sea clutter. Hence, radar systems operating in these environments would benefit from knowing the effects of the environment on their system performance. This requires the knowledge of atmospheric refractivity and refractivity-from-clutter (RFC) refers to techniques that estimate this refractivity profile from the increased radar clutter returns by matching the split-step fast Fourier transform (FFT) parabolic equation (PE) simulated clutter pattern of a candidate environment with the radar measured clutter pattern [1–4]. For more discussion on different RFC techniques see [3]. However, radar system parameters, particularly the radar height and frequency affects the RFC performance significantly. For lower frequencies (*e.g.* a typical S-band radar such as the Space Range Radar (SPANDAR)) the clutter decreases monotonically with range. This quickly changes as the frequency is increased especially for environments with large EDH values. Higher antenna heights also tend to have clutter libraries (See [1]) with monotonically decreasing clutter. However, it also results in similar clutter signatures for different evaporation duct heights (EDH). Moreover, if the antenna is too high above the duct, it may not sufficiently excite the duct, resulting in a drop in the available clutter-to-noise ratio (CNR). This complex relationship between RFC performance, frequency and the antenna height is studied for typical naval radar heights from 5 to 50 m, and three frequency bands, namely S, C, and X-bands covering 2–12 GHz. Finally, the paper also covers how to find the best RFC system parameters and how to create performance maps of the region of interest. Factors such as the complex local and global atmospheric processes, proximity to land, and latitude differences result in regions with very different duct statistics. Different RFC inversion systems will have different EDH intervals within which they will perform best.

## 2 RFC Performance Analysis

The complex signal $y(r_k)$ received by the radar in non-standard propagation conditions can be computed by $y(r_k) = c r_k^{1/2} L^{-1}(r_k)\sqrt{\sigma^o(r_k)} + w(r_k)$, where $r_k$ is the range of the $k$th radar range bin, $w(r_k)$ is the additive complex Gaussian noise, and $\sqrt{\sigma^o(r_k)}$ represents the complex sea clutter amplitude, $L$ is the one-way propagation loss computed by the FFT-PE, and $c$ represents the collection of constant terms. The evaporation duct estimation algorithm given in [1] is analyzed here with a CNR at 10 km of 40 dB (SPANDAR specifications) and a mildly spiky K-distributed sea clutter with a shape parameter of $\nu = 1$. The six cases (Env-1 to Env-6) investigated here are given in Fig. 1. Selected regions, seasons, and time of

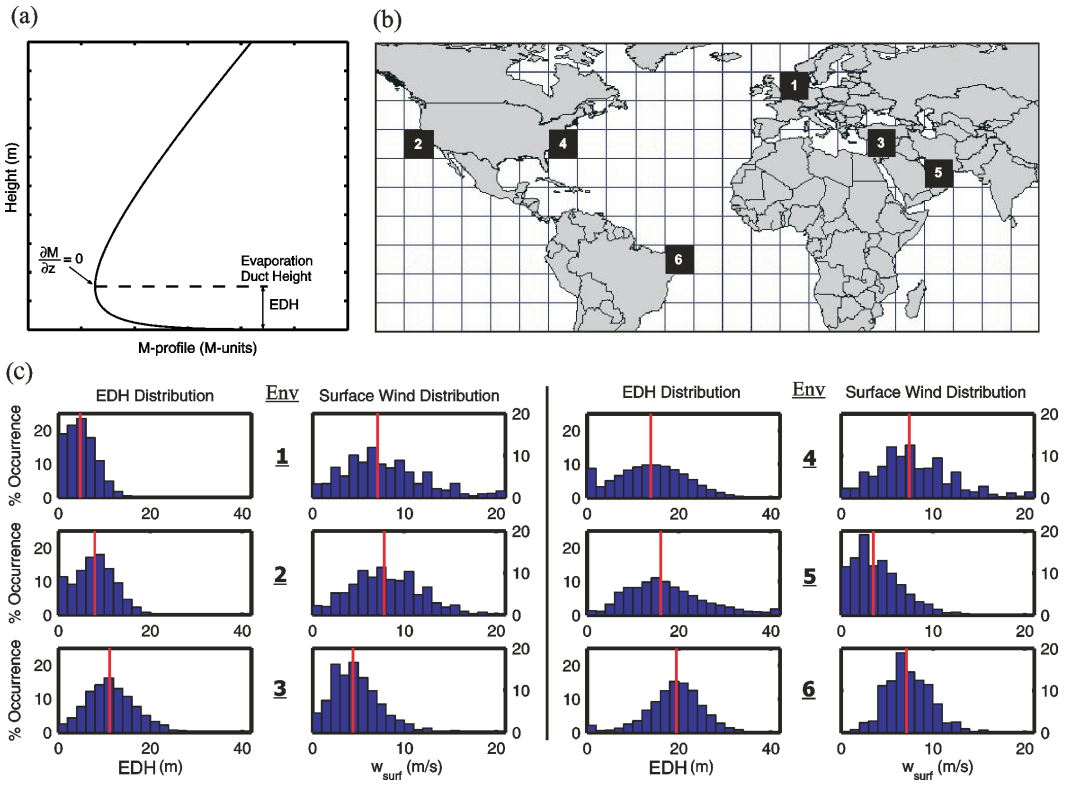


Figure 1: (a) The vertical refractivity profile for an evaporation duct, (b) Marsden squares of the six regions used in the simulations, and (c) the EDH and surface wind speed pdfs of these regions.

day information is provided in Table 1 along with the mean EDH and surface wind speed values. They are selected such that they represent a wide spectrum of environments with different mean and statistics for the EDH, and hence different RFC performance. The cases are ranked according to their mean EDHs.

This nonlinear performance characteristic (given as RMS error in EDH) can be seen in Fig. 2. Each plot shows how radar systems with different frequencies (2–12 GHz) and antenna heights (5–50 m) will perform for a given EDH. For small EDH values, most frequency-height combinations work well. As EDH increases certain regions perform better than others and these regions shift with EDH except for the low frequency-low radar height combination. Also note that regions with poor performance start to appear as early as a duct height of only 5 m. Since the performance of each frequency-height value depends on the actual EDH of the environment it is operating in, regional statistics also must be incorporated to give a true performance metric for a RFC system.

Table 1: Regional Environmental Statistics

| Env. | MS | Region | Season | Time | Mean EDH (m) | Mean $V_{wind}$ (m/s) |
|---|---|---|---|---|---|---|
| Env-1 | MS-216 | North Sea | Spring | Day | 4.8 | 7.1 |
| Env-2 | MS-121 | Coast of Calif. | Summer | Night | 7.9 | 7.8 |
| Env-3 | MS-141 | East Mediter. | Spring | Day | 11.2 | 4.8 |
| Env-4 | MS-116 | Wallops Island | Spring | Day | 13.9 | 7.4 |
| Env-5 | MS-103 | Persian Gulf | Fall | Day | 16.1 | 3.5 |
| Env-6 | MS-303 | Coast of Brazil | Fall | Day | 19.5 | 7.1 |

Regional statistics can be incorporated into the performance by weighing the EDH RMS error with the pdf of the EDH $\mathrm{p}(h_\mathrm{d})$ in that region/season/time of the day. Hence, the error metric $e(f, z_\mathrm{a})$ can be given by

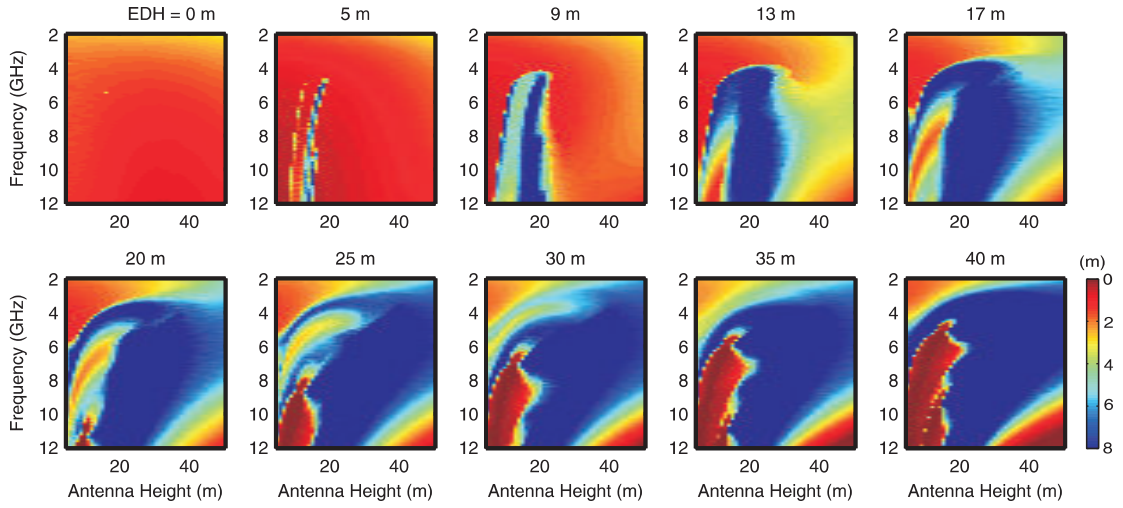


Figure 2: Performance plots: RMS evaporation duct height error as a function of radar frequency and antenna height in environments with duct heights ranging from 0 to 40 m.

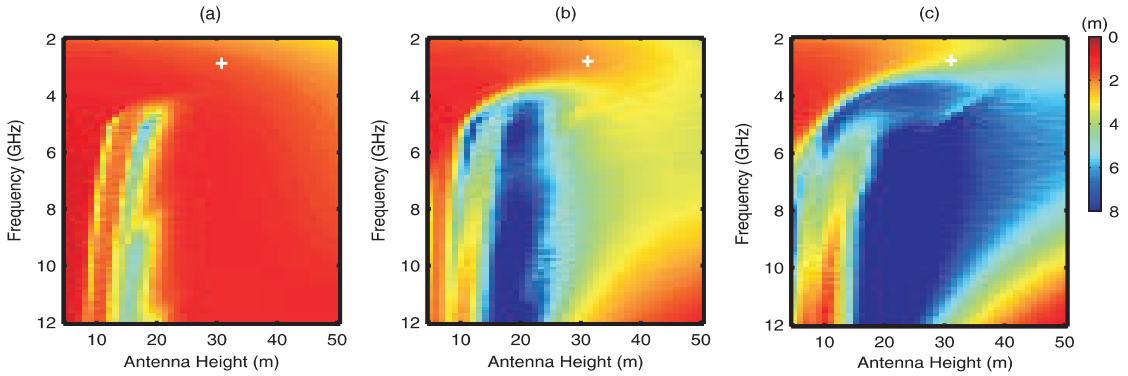


Figure 3: Performance plots: RMS error integrated over the regional statistics: (a) Env-1, (b) Env-3, and (c) Env-6. The '+' indicates the frequency and the antenna height of the Space Range Radar (SPANDAR).

$e(f, z_{\mathrm{a}}) = \int_{h_{\mathrm{d}}} \sqrt{\mathrm{E}\left[\left(\widehat{h}_{\mathrm{d}}(f, z_{\mathrm{a}}) - h_{\mathrm{d}}\right)^2\right]}\, \mathrm{p}(h_{\mathrm{d}}) dh_{\mathrm{d}}$, where $f$ and $z_{\mathrm{a}}$ are the radar frequency and antenna height.

The performance plots of three environments selected from Table 1 are given in Fig. 3. Comparing Fig. 3(a) with Fig. 3(c), it can be concluded that RFC performance is a strong function of the regional statistics. Most frequency-height combinations work well in Env-1 whereas they must be selected carefully for Env-6. For example, the SPANDAR radar ('+' in Fig. 3 at 2.8 GHz, 31 m) seems to be a good choice for Env-1 and Env-3 but performance is only mediocre in Env-6. RMS error of all 6 environments (Table 1) for 5 different frequency–heights are given in Table 2. The low frequency–low height system gives the best RMS errors for all 6 environments with a small variation in performance from region to region. On the contrary, the RMS error of the 8 GHz system varies from 2.3 m to 11.2 m. Also note how SPANDAR performs better in the first three environments, whereas the 10 GHz, 10 m system works better in the last three.

The final example shows a RFC performance map of the larger Mediterranean/Arabian Sea Region for the SPANDAR radar (Fig. 4). Day/night averaged annual statistics for each Marsden Square (MS) are used to compute the performance and values between are interpolated. Some noticeable features are the large RMS error in the Red Sea, larger errors in Indian Ocean with respect to the Eastern Atlantic Ocean

Table 2: RMS Error in Meters of Five Frequency-Height Values for the Environments given in Table 1.

| RMS Error (m) | 2.8 GHz 31 m | 3 GHz 10 m | 6 GHz 15 m | 8 GHz 20 m | 10 GHz 10 m |
|---|---|---|---|---|---|
| Env-1 | 1.8 | 1.3 | 2.3 | 2.3 | 1.9 |
| Env-2 | 1.9 | 1.3 | 3.6 | 5.4 | 2.6 |
| Env-3 | 2.2 | 1.3 | 4.5 | 8.6 | 2.9 |
| Env-4 | 2.7 | 1.5 | 4.1 | 8.8 | 2.4 |
| Env-5 | 3.1 | 1.5 | 4.4 | 10.0 | 2.4 |
| Env-6 | 3.5 | 1.6 | 4.3 | 11.2 | 2.2 |

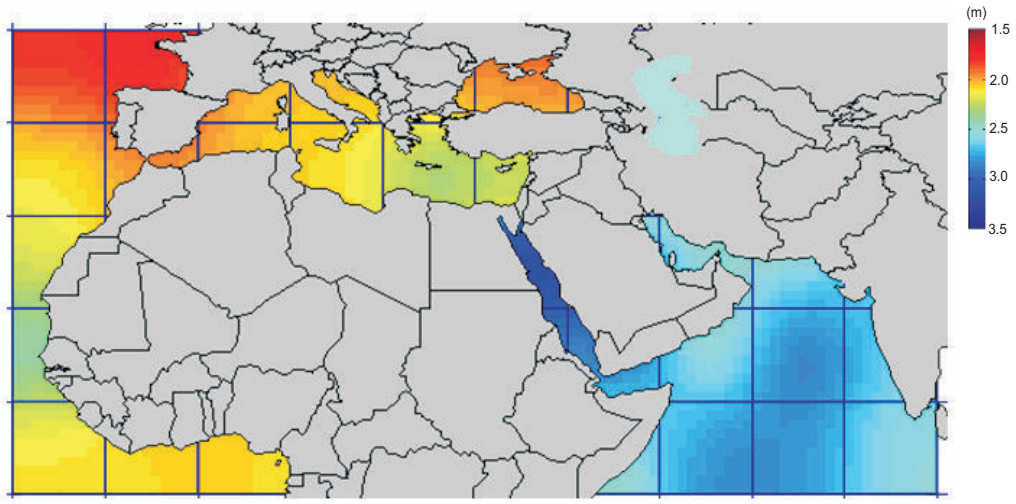


Figure 4: Performance map of the East Atlantic Coast, Mediterranean, Persian Gulf, Red Sea, Black Sea, and the Arabian Sea. RMS evaporation duct height error for SPANDAR.

with similar latitudes, and decreasing performance from West to East Mediterranean. Note the correlation between the performance pattern and the mean EDH (from west to east: 9.8, 10.6, 11.3, 12.5, and 12.4 m) of the regional statistics in the Mediterranean.

## 3 Conclusion

In this paper, the performance of a clutter-based evaporation duct estimator was calculated. The effects of antenna height, and frequency were shown. Performance map were created by incorporating the regional meteorological statistics.

## 4 Acknowledgment

This work was supported by the Office of Naval Research Code 32, under grant N00014-05-1-0369.

## References

[1] L. T. Rogers, C. P. Hattan, and J. K. Stapleton, "Estimating evaporation duct heights from radar sea echo," *Radio Science*, vol. 35 (4), pp. 955–966, 2000, doi:10.1029/1999RS002275.

[2] C. Yardim, P. Gerstoft, and W. S. Hodgkiss, "Estimation of radio refractivity from radar clutter using Bayesian Monte Carlo analysis," *IEEE Trans. Antennas Propagat.*, vol. 54(4), pp. 1318–1327, 2006.

[3] ——, "Statistical maritime radar duct estimation using a hybrid genetic algorithm – Markov chain Monte Carlo method," *Radio Science*, vol. 42, 2007, doi:10.1029/2006RS003561.

[4] ——, "Tracking refractivity from clutter using Kalman and particle filters," *IEEE Trans. Antennas Propagat.*, to appear, 2008.